

# Cobalt and Iron Stabilized Ketyl, Ketiminyl and Aldiminyl Radical Anions

Grégoire Sieg,<sup>[a]</sup> Quentin Pessemesse,<sup>[b, c]</sup> Sascha Reith,<sup>[a]</sup> Stefan Yelin,<sup>[e]</sup> Christian Limberg,<sup>[e]</sup> Dominik Munz,<sup>[c, d]</sup> and C. Gunnar Werncke<sup>\*[a]</sup>

**Abstract:** Carbonyl and iminyl based radical anions are reactive intermediates in a variety of transformations in organic synthesis. Herein, the isolation of ketyl, and more importantly unprecedented ketiminyl and aldiminyl radical anions coordinated to cobalt and iron complexes is presented. Insights into the electronic structure of these unusual

metal bound radical anions is provided by X-Ray diffraction analysis, NMR, IR, UV/Vis and Mössbauer spectroscopy, solid and solution state magnetometry, as well as a by a detailed computational analysis. The metal bound radical anions are very reactive and facilitate the activation of intra- and intermolecular C–H bonds.

## Introduction

The metal-mediated reduction of ketones and aldehydes is a well-known synthetic methodology. It can be employed for substrate deoxygenation (Clemmensen reduction, Zn) or for the construction of 1,2-diols (pinacol coupling; Mg, SmI<sub>2</sub> or low valent early transition metal complexes) and olefins (McMURRAY-Coupling, Ti).<sup>[1,2,3]</sup> Similarly, ketimines and aldimines may be reduced leading to 1,2-diamines.<sup>[2]</sup> In these, and in other reactions such as the amide reduction to alcohols,<sup>[4]</sup> the initial substrate reduction via the formation of metal-bound radical anions supposedly is the key step, which concurs with the umpolung of the electrophilic carbonyl carbon atom. In recent

years, the importance of these and other radical anions further emerged due to their role as crucial intermediates in photo-redox catalysis.<sup>[3,5]</sup> Hitherto, experimental insights into those radical anions is essentially restricted to in situ EPR- and UV/Vis spectroscopic data.<sup>[6]</sup> Another way to expand the knowledge of these radical anions is by isolation of their metal complexes. However, examples for metal-bound carbonyl or iminyl radical anions are scarce and mostly restricted to diaryl ketones as illustrated for the isolation of the alkali metal salts the benzophenone or fluorenone radical anion.<sup>[7,8]</sup>

Few additional examples of other metal complexes bearing simple diaryl ketyl or fluorenyl radical anions were authenticated in case of transition- (Fe, Zr)<sup>[9–11]</sup> and rare earth metals (Sm, Eu, Yb, La)<sup>[12,13–16]</sup> as well as uranium<sup>[17]</sup> and alkali (earth) metals.<sup>[18,19]</sup> Here, the intermolecular coupling of the substrate occurs in the absence of sufficient steric protection or blocking of susceptible substrate positions, which in rare cases is found to be reversible. The coupling occurs under pinacol coupling or Gomberg-type dimerization, as expected from the behaviour of free radical anions.<sup>[11,13–17,20,21]</sup> Recently, these endeavours were extended to organic amides using a highly reducing U<sup>III</sup> complex.<sup>[21]</sup> In contrast, complexes with aldehyde radical anions or related “simple” imine derivatives such as aldimines (R(H)NH) and ketimines (R<sub>2</sub>NH) are absent in the literature. This is surprising given the reversible redox chemistry (viz. redox activity) of ubiquitous imino containing ligands including α-diimines, α-iminopyridines or pyridino diimines (PDIs).<sup>[22]</sup>

Herein, we present the isolation of rare examples of metal\*stabilized ketyl radical anions as well as unique ketiminyl and aldiminyl radical anions using the quasilinear cobalt(I) and iron(I) complexes K<sub>m</sub>[M(N(SiMe<sub>3</sub>)<sub>2</sub>)<sub>2</sub>] (m = 18c6, crypt.222) as reductants and coordination site (Figure 1). The radical anionic nature of the substrates L in the K<sub>m</sub>[M(L<sup>•-</sup>)(N(SiMe<sub>3</sub>)<sub>2</sub>)<sub>2</sub>] complexes was proven via thorough characterization using X-Ray diffraction (XRD) analysis, <sup>1</sup>H-, IR-, EPR- (for cobalt), Mössbauer (for iron) and UV/Vis spectroscopy, cyclic voltammetry as well as magnetic measurements in comparison to the neutral metal(II) adducts. Quantum chemical calculations at the

[a] G. Sieg, S. Reith, Dr. C. G. Werncke

Fachbereich Chemie  
Philipps-Universität Marburg  
Hans-Meerwein-Straße 4, 35043 Marburg (Germany)  
E-mail: gunnar.werncke@chemie.uni-marburg.de

[b] Q. Pessemesse

Univ. Lyon, ENS de Lyon, CNRS UMR 5182  
Université Claude Bernard Lyon 1, Laboratoire de Chimie  
69342, Lyon (France)

[c] Q. Pessemesse, Prof. Dr. D. Munz

Anorganische Chemie: Koordinationschemie  
Campus C4.1  
Universität des Saarlandes 66123 Saarbrücken (Germany)

[d] Prof. Dr. D. Munz

Department Chemie und Pharmazie  
Friedrich-Alexander Universität (FAU) Erlangen-Nürnberg  
Egerlandstr. 1, D-91058 Erlangen (Germany)

[e] S. Yelin, Prof. Dr. C. Limberg

Institut für Chemie  
Humboldt-Universität zu Berlin  
Brook-Taylor-Str. 2, 12489 Berlin (Germany)

Supporting information for this article is available on the WWW under <https://doi.org/10.1002/chem.202103096>

© 2021 The Authors. Chemistry - A European Journal published by Wiley-VCH GmbH. This is an open access article under the terms of the Creative Commons Attribution Non-Commercial NoDerivs License, which permits use and distribution in any medium, provided the original work is properly cited, the use is non-commercial and no modifications or adaptations are made.

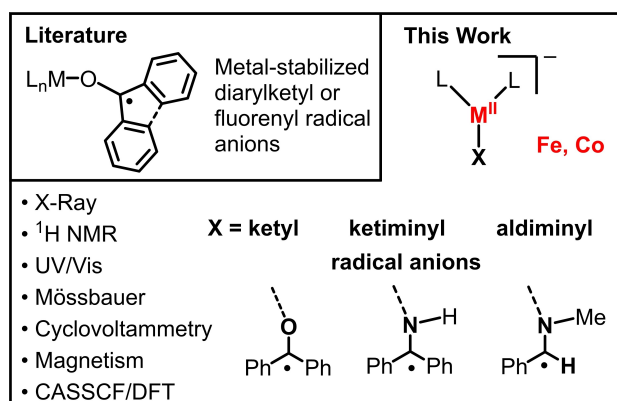


**Figure 1.** Metal-stabilized ketyl, ketiminyl and aldiminyl radical anions in the literature and in this report.

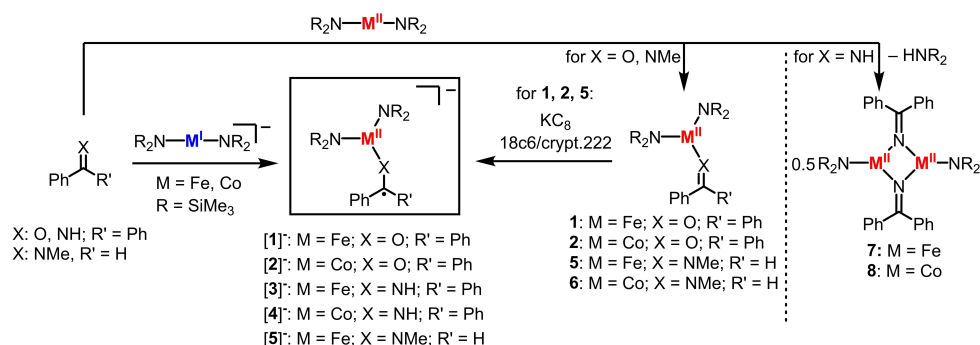
density functional theory (DFT) as well as NEVPT2/CASSCF level of theory further corroborate this picture. The radical anion complexes undergo varied bond activation chemistry.

## Results and Discussion

### Synthesis and structure

Addition of benzophenone (bp) to the quasilinear iron(I) and cobalt(I) complexes  $K\{m\}[M^I(N(SiMe_3)_2)_2]$  ( $m = 18\text{-crown-6}$  or crypt.222)<sup>[23–25]</sup> resulted immediately in intensely blue and violet colored solutions from which  $K\{m\}[Fe(bp)(N(SiMe_3)_2)_2]$ ,  $K\{m\}[1]$ , and  $K\{m\}[Co(bp)(N(SiMe_3)_2)_2]$ ,  $K\{m\}[2]$  were isolated (Scheme 1). The analogous, yet more challenging, reduction of aldehydes and the related ketimines and aldimines was attempted as well. Whereas only colorless unidentifiable products were obtained for acetaldehyde, which arguably indicates substrate coupling, ketimine benzophenone imine (bpi) allowed to isolate turquoise  $K\{m\}[Fe(bpi)(N(SiMe_3)_2)_2]$ ,  $[3]^-$ , and  $K\{m\}[Co(bpi)(N(SiMe_3)_2)_2]$ ,  $[4]^-$ . Both bpi-complexes decompose rapidly ( $t_{1/2} \approx 5$  min.) at room temperature and could therefore only be analysed via XRD and in situ UV/VIS spectroscopy. The analogous reaction of the aldimine benzaldehyde methylamine (bama) with the metal (I) precursors led in case of iron to the formation of dark yellow  $K\{m\}[Fe(bama)(N(SiMe_3)_2)_2]$ , **5**. In contrast, no reaction was observed for the reaction of the cobalt(I) complex with bama.

For comparison, the synthesis of the neutral metal(II) substrate adducts was pursued as well.  $[M(N(SiMe_3)_2)_2]$  readily formed adducts with bama and bp, whereas for bpi unproductive substrate deprotonation and formation of dimeric complexes  $[(M(N(SiMe_3)_2)_2)(\mu\text{-NCPH}_2)_2]$  (Fe: **7**, Co: **8**) was observed. The metal(II) adducts **1**, **2** and **5** could also be used for the



**Scheme 1.** Synthesis of iron and cobalt ketyl-, ketiminyl- and aldiminyl radical anion complexes  $[1]^-$ – $[5]^-$  and neutral complexes **1**, **2**, **5** and **6**.

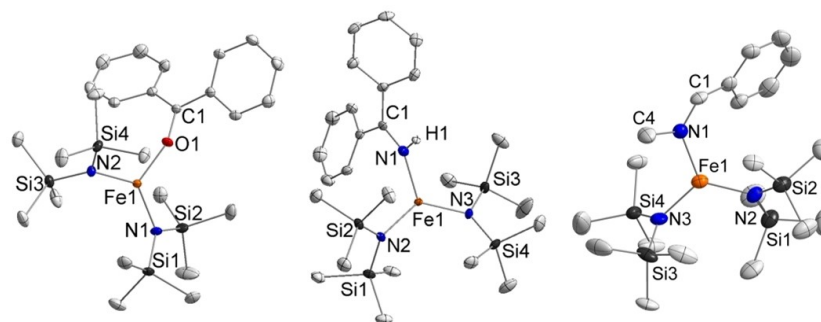


**Figure 2.** Molecular structures of the complex anions of compounds  $K\{m\}[1]$ ,  $K\{m\}[3]$  and  $K\{m\}[5]$ . H atoms (except H1) and  $[K\{18c6\}]^+$  cations are omitted for clarity and ellipsoids are shown at 50% probability.

formation of their reduced counterparts, with the exception of **6**. There, the reduction with  $\text{KC}_8$  led to the formation of the adduct free  $[\text{Co}^{\text{I}}(\text{N}(\text{SiMe}_3)_2)_2]^-$ . This indicates that the aldiminyl radical anion is more reducing than the cobalt ion which is in line with indifference of bama towards the cobalt(I) complex.

X-ray diffraction analysis of the anionic, trigonal planar iron and cobalt benzophenone complexes revealed C–O bond lengths of 1.310(2) Å ( $[\text{1}]^-$ ) and 1.324(2) Å ( $[\text{2}]^-$ ) (Figure 1). In comparison to those found for their respective, neutral counterparts (1.248(9) Å (**1**) and 1.244(2) Å (**2**)) as well as for other authenticated ketyl radical anion complexes,<sup>[9–11,17,18]</sup> this hints at the presence of a ketyl radical anion.

Accordingly, the M–O bonds of 1.869(1) Å ( $[\text{1}]^-$ ), 1.903(1) Å ( $[\text{2}]^-$ ) are considerably shorter than those of their neutral counterparts (**1** (bp): 2.025(5) Å, **5** (bama): 2.119(2) Å). This is similar to the only other late 3d-metal ketyl complex. (Fe(II)–O 1.8565(10) Å)<sup>[9]</sup> and in the general range found for anionic O-donor ligands. The iron benzophenone imine complex  $[\text{3}]^-$  exhibits an Fe–N<sub>bpi</sub> bond length of 1.917(2) Å with N<sub>bpi</sub>–C distance of 1.299(3) Å. For  $[\text{4}]^-$  both the Co–N<sub>bpi</sub> (1.946(2) Å) and the N<sub>bpi</sub>–C bonds are longer (1.350(4) Å) (Table 1). While the value of N<sub>bpi</sub>–C of  $[\text{4}]^-$  is comparable to cobalt(II) complexes of monoreduced aryliminopyridines (approx. 1.34 Å),<sup>[26]</sup> the N<sub>bpi</sub>–C distance of the iron complex  $[\text{3}]^-$  is surprisingly short.<sup>[27]</sup> However, the very short Fe–N<sub>bpi</sub> bond implicated an anionic amide ligand which gave overall an ambiguous picture for  $[\text{3}]^-$  on a structural level. The comparison of the structural metrics for the iron aldimine complexes  $[\text{5}]^-$  and **5** show clearly longer N<sub>bama</sub>–C bond (1.331(6) Å) and shorter Fe–N<sub>bama</sub> bond (1.978(4) Å) for the reduced complex  $[\text{5}]^-$  (**5**: Fe–N<sub>bama</sub> 2.0119(2) Å; N<sub>bama</sub>–C 1.275(3) Å). The average M–N<sub>SiMe3</sub> bond lengths of all reduced complexes are slightly elongated (Fe: 1.95–1.97 Å; Co: 1.93–1.97 Å) in comparison to the neutral counterparts (Fe: 1.91–1.94 Å; Co: 1.90–1.92 Å).

The electrochemical behaviour of all isolable mononuclear compounds was investigated by cyclic voltammetry (Figures S41–S44). The anionic compounds exhibited no meaningful redox events, a phenomenon already observed for other anionic, low-valent 3d-metal silylamides with radical anionic ligands.<sup>[28]</sup> In contrast, for the neutral compounds **1** and **2** a reversible reduction at  $E_{1/2} = -2.06$  V (**1**) and  $E_{1/2} = -2.10$  V (**2**) was observed (200 mVs<sup>-1</sup>, vs. Fc/Fc<sup>+</sup> propylene carbonate). For **5** the reduction is irreversible ( $E_{p/2} = -2.83$  V (**5**)). These reduction potentials are suspiciously similar to those of the free

substrates, which is indicative for a substrate-centred reduction although we cannot fully rule out substrate dissociation under the CV conditions.

## Spectroscopy

UV/Vis spectroscopic examination of the anionic iron ketyl and ketiminyll complexes show distinct absorption maxima at 581 nm ( $[\text{1}]^-$ ) and 567 nm ( $[\text{3}]^-$ ) (Figure 3 and Table 2), which is consistent with previously reported ketyl-radical anions.<sup>[7,9,11,17]</sup> We attribute these features on the basis of TD-DFT (Table S11, Figure S60–S70) and state averaged CASSCF/NEVPT2 (Table S12–S15, Figure S76–78) calculations to the  $\pi$ - $\pi^*$  transitions, which share considerable metal-to-ligand charge-transfer (MLCT) character. Similarly, the analogous cobalt compounds exhibit absorption maxima at 567 nm ( $[\text{2}]^-$ ) and 594 nm ( $[\text{4}]^-$ ). The aldiminyl radical iron complex  $[\text{5}]^-$  lacks any absorption in this region, but exhibits a pronounced absorption at 486 cm<sup>-1</sup>. The blue-shift is likely due to the absence of the second aryl substituent and thus overall smaller aromatic system. For comparison, the neutral metal substrate adducts exhibit no such absorption bands.

<sup>1</sup>H NMR spectroscopic examination of the reduced, stable complexes  $[\text{1}]^-$ ,  $[\text{2}]^-$ , and  $[\text{5}]^-$  revealed extensive paramagnetic features. The position of the respective SiMe<sub>3</sub> signals (Fe:  $[\text{1}]^-$ : -2.56 ppm,  $[\text{5}]^-$ : -3.02 ppm; Co:  $[\text{2}]^-$ : -12.47 ppm) resembles those of comparable trigonal metal(II) complexes (e.g. [Fe(N(SiMe<sub>3</sub>)<sub>2</sub>)<sub>2</sub>(F)]<sup>-</sup>: -2.29 ppm),<sup>[29]</sup> ([Co(NH<sup>t</sup>Bu)(N(SiMe<sub>3</sub>)<sub>2</sub>)<sub>2</sub>]<sup>-</sup>: -15.45 ppm<sup>[23]</sup>). As the SiMe<sub>3</sub> signal is highly sensitive to the coordination environment and oxidation state, it would support the notion of three-coordinate metal(II) ions in all these compounds. Interestingly, upon dissolution of otherwise analytical pure  $[\text{2}]^-$  the presence of precursor complex [K(18c6)][Co(N(SiMe<sub>3</sub>)<sub>2</sub>)<sub>2</sub>] could be detected. Addition of further amounts of benzophenone did not fully suppress the signal belonging to the cobalt(I) starting compound (and also initiated partial

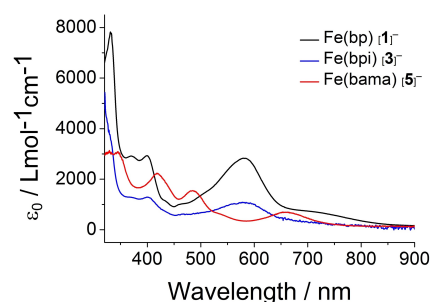


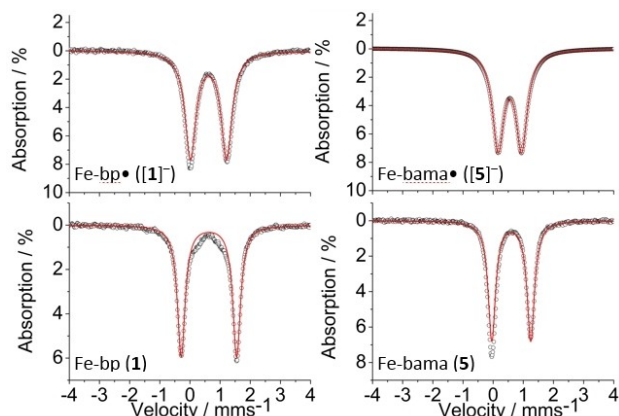
Figure 3. UV-Vis spectra of complexes  $[\text{1}]^-$ ,  $[\text{3}]^-$  and  $[\text{5}]^-$  in  $\text{Et}_2\text{O}$ .

Table 1. Selected structural metrics of complexes  $[\text{1}]^-$ – $[\text{5}]^-$ , **1**, **2**, **5** and **6**.

Compound	M–X/Å	C–X/Å	M–N1/Å	M–N2/Å
Fe(bp*) ( $[\text{1}]^-$ )	1.869(1)	1.310(2)	1.951(1)	1.953(1)
Co(bp*) ( $[\text{2}]^-$ )	1.903(1)	1.324(2)	1.960(1)	1.934(1)
Fe(bpi*) ( $[\text{3}]^-$ )	1.917(2)	1.299(3)	1.965(2)	1.966(2)
Co(bpi*) ( $[\text{4}]^-$ )	1.946(2)	1.350(4)	1.954(2)	1.971(2)
Fe(bama*) ( $[\text{5}]^-$ )	1.978(4)	1.331(6)	1.971(4)	1.968(4)
Fe(bp) ( <b>1</b> )	2.025(5)	1.248(9)	1.937(6)	1.912(6)
Co(bp) ( <b>2</b> )	2.025(1)	1.244(2)	1.899(1)	1.903(2)
Fe(bama) ( <b>5</b> )	2.119(2)	1.275(3)	1.934(2)	1.930(2)
Co(bama) ( <b>6</b> )	2.061(2)	1.276(4)	1.905(2)	1.916(2)

Table 2. UV/Vis-spectroscopic characteristics of  $[\text{1}]^-$ – $[\text{5}]^-$ .

	Fe(bp*) [1]-	Fe(bpi*) [3]-	Fe(bama*) [5]-	Co(bp*) [2]-	Co(bpi*) [4]-
$\lambda_{\text{max}}$ / nm	581	584	486	567	594
$\epsilon_0$ / L mol <sup>-1</sup> cm <sup>-1</sup>	2830	1080	1550	3720	n.a.



**Figure 4.**  $^{57}\text{Fe}$ -Mössbauer spectra of  $\text{K}(18\text{c}6)[1]^-$  (top left), **1** (bottom left),  $\text{K}(18\text{c}6)[5]^-$  (top right) and **5** (bottom right) at 15 K. Isomer shifts  $\delta$  and quadrupole splittings  $\Delta Q$  are as following:  $[1]^-$ :  $\delta = 0.62 \text{ mms}^{-1}$ ,  $\Delta Q = 1.20 \text{ mms}^{-1}$ ; **1**:  $\delta = 0.62 \text{ mms}^{-1}$ ,  $\Delta Q = 1.83 \text{ mms}^{-1}$ ;  $[5]^-$ :  $\delta = 0.56 \text{ mms}^{-1}$ ,  $\Delta Q = 0.78 \text{ mms}^{-1}$ ; **5**:  $\delta = 0.58 \text{ mms}^{-1}$ ,  $\Delta Q = 1.31 \text{ mms}^{-1}$ .

decomposition via detection of  $[\text{Co}(\text{N}(\text{SiMe}_3)_2)_3]^-$ , which points to an equilibrium between  $[2]^-$  and starting complex/free benzophenone. A similar observation was already made by us for the cobalt alkyne complex  $[\text{Co}(\eta^2\text{-PhCCPh})(\text{N}(\text{SiMe}_3)_2)_2]^{[30]}$  which we attribute in the present case also to the low reduction potential of  $[\text{Co}(\text{N}(\text{SiMe}_3)_2)_2]$  ( $E_{\text{red}} = -1.47 \text{ V}$ ).<sup>[25]</sup>

For more intimate insights into the electronic situation,  $^{57}\text{Fe}$  Mössbauer (for iron) and EPR spectroscopy (for cobalt) was performed. All iron compounds **1**,  $[1]^-$ , **5** and  $[5]^-$  (Figure 4, S53–56), show doublets with similar isomer shifts ( $0.56$ – $0.62 \text{ mms}^{-1}$ ) in the Mössbauer spectra. These values correspond well with those observed for related trigonal planar high-spin iron(II) complexes ( $[\text{Fe}(\text{NR}_2)_2]^-$ :  $\delta = 0.63 \text{ mms}^{-1}$ ;  $[\text{Fe}(\text{NR}_2)_3]^-$ :  $\delta = 0.59 \text{ mms}^{-1}$ )<sup>[24,31]</sup> which speaks to a divalent metal ion in all compounds presented herein. The measured quadrupole splittings are smaller for the reduced complexes ( $0.78$ – $1.20 \text{ mms}^{-1}$ ) than for the neutral counterparts ( $1.31$ – $1.83 \text{ mms}^{-1}$ ). This can be reasoned by the more pseudo- $C_3$ -symmetric geometry of the reduced compounds.

For the cobalt complex  $[2]^-$  X-Band EPR-spectroscopy showed at 4 K broad absorptions at  $g \approx 10$  and 3.84 and as well as a very sharp signal at  $g = 2.00$  (Figure S57). The broad features are indicative of an axial signal corresponding to a high-spin cobalt(II) ion.<sup>[32]</sup> This becomes more evident as these signals disappear above 80 K (Figure S58). The signal at  $g = 2.00$  likely belongs to the ketyl centred radical whereas its sharp, isotropic form suggests rather weak delocalisation of the electron over the cobalt ion.<sup>[21,33]</sup>

## Magnetism

For further insights into the electronic structure of the anionic complexes, namely the iron complexes  $[1]^-$ ,  $[5]^-$  as well as the cobalt complex  $[2]^-$ , their magnetic features in the solid state and solution (Evans method) were probed (Figure 5). The

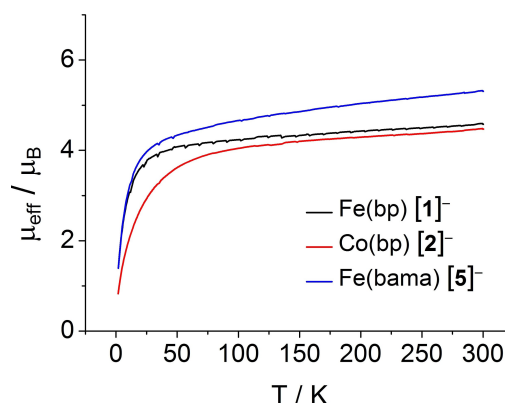


**Figure 5.** Temperature dependent magnetic susceptibility ( $\chi T$  vs.  $T$ ) for **1**, **2** and **5** from 3 K to 300 K

effective magnetic moments of the iron complexes amount to  $\mu_{\text{eff}} = 4.92 \mu_B$  ( $[1]^-$ ) and  $\mu_{\text{eff}} = 4.65 \mu_B$  ( $[5]^-$ ) in solution, which is in good agreement to the values found in the solid state at 300 K ( $[1]^-$ :  $\mu_{\text{eff}} = 4.40 \mu_B$ ;  $[5]^-$ :  $\mu_{\text{eff}} = 4.67 \mu_B$ ). The  $\chi_m T$  vs.  $T$  slopes of these compounds decrease steadily down to 50 K where a sharper drop is observed (Figure 5). Under the premise of an iron(II) ion interacting with an organic radical the observed values for both compounds lie between the theoretical spin-only values expected for a ferromagnetically coupled ( $5.19 \mu_B$ ) system and for strong antiferromagnetic coupling ( $3.87 \mu_B$ ). Further, these values are higher than those of low-coordinate high-spin iron(II) complexes, which would be the hypothetical case of a non-reduced substrate.<sup>[34]</sup> The presence of antiferromagnetic coupling also explains that the curves do not plateau at higher temperatures. Similar conclusions can be drawn for the cobalt complex  $[2]^-$  (solution:  $\mu_{\text{eff}} = 4.43 \mu_B$ ; solid state, 300 K:  $\mu_{\text{eff}} = 4.75 \mu_B$ ). Its values are higher than the one of the cobalt(II) precursor ( $\mu_{\text{eff}} = 4.21 \mu_B$ )<sup>[25]</sup> and the spin-only value of a cobalt(II) ion with antiferromagnetic coupling to the radical anion ( $S = 1$ ;  $2.83 \mu_B$ ) but lower than the alternative of ferromagnetic coupling ( $S = 2$ ;  $4.90 \mu_B$ ). Considering the general presence of significant spin-orbit contributions for cobalt(II) ions this speaks for an antiferromagnetically coupled system in  $[2]^-$ .

## Quantum chemical calculations

In order to further pinpoint the electronic structure of the anionic complexes  $[1]^-$ – $[5]^-$  as well as the neutral congeners **1**, **2**, and **5**, scalar relativistic (ZORA) quantum chemical calculations were performed.<sup>[35]</sup> Various methods (CASSCF/NEVPT2; PBE, BP86, PBE0, TPSS, TPSSh, B3LYP, M06, PBEh-3c, B97-3c) were applied, which all gave qualitatively consistent results. Overall, all complexes  $[1]^-$ – $[5]^-$  contain a high-spin metal ion anti-ferromagnetically coupled to a ligand centred radical (Table S8–16). For instance, the benzophenone coordinated iron

complex  $[1]^-$  features a  $d^6$  configured iron centre in the oxidation state +II with overall  $S=3/2$  (Figure 6).<sup>1</sup>

Thereof, the  $d(z^2)$  orbital is doubly occupied. The ligand centred radical is mainly located at the carbonyl carbon atom in the  $p(y)$  orbital (Table S10). It is moderately delocalized over the two phenyl substituents, and mixes with the  $d(xy)$  orbital. The NEVPT2/CASSCF (Table S15) calculations<sup>[36]</sup> predict a vertical quartet–sextet gap  $\Delta E^{q/s}$  of 0.16 eV, which is well reproduced by both vertical as well as adiabatic values from the DFT calculations (PBE<sup>adiabatic</sup>:  $\Delta E^{q/s} = 24 \text{ kJ mol}^{-1}$ ; PBE<sup>vertical</sup>:  $\Delta E^{q/s} = 25 \text{ kJ mol}^{-1}$ ). Accordingly, the cobalt complex  $[2]^-$  can be understood as a  $d^7$  configured cobalt centre with doubly occupied  $d(z^2)$  and  $d(xz)$  orbitals, and an anti-ferromagnetically coupled radical ligand, leading to a  $S=1$  spin system (Figure S80). The triplet–quintet gap  $\Delta E^{t/q}$  is predicted to be 0.12 eV (PBE<sup>adiabatic</sup>:  $\Delta E^{t/q} = 21 \text{ kJ mol}^{-1}$ ; PBE<sup>vertical</sup>:  $\Delta E^{t/q} = 30 \text{ kJ mol}^{-1}$ ). While anionic complexes  $[1]^-$  to  $[5]^-$  display ligand-centered radicals, the iminyl and aldiminyl ligands bear slightly reduced spin-density on the carbon atom (Table S10).

Contrarily, the carbonyl- and imine ligand in the neutral metal complexes are all redox-innocent and coordinate the high-spin metal centres (Table S19). This picture is not only consistent with the experimental (see above) and computed C=X bond lengths, but manifests as well in the C–X stretches (Table 3). Whereas their intensity is too low to allow for an unambiguous identification experimentally (Figure S82), they were extracted from the computational data (Table S16). The stretches in  $[1]^-$ – $[5]^-$  occur at lower wave numbers in reference

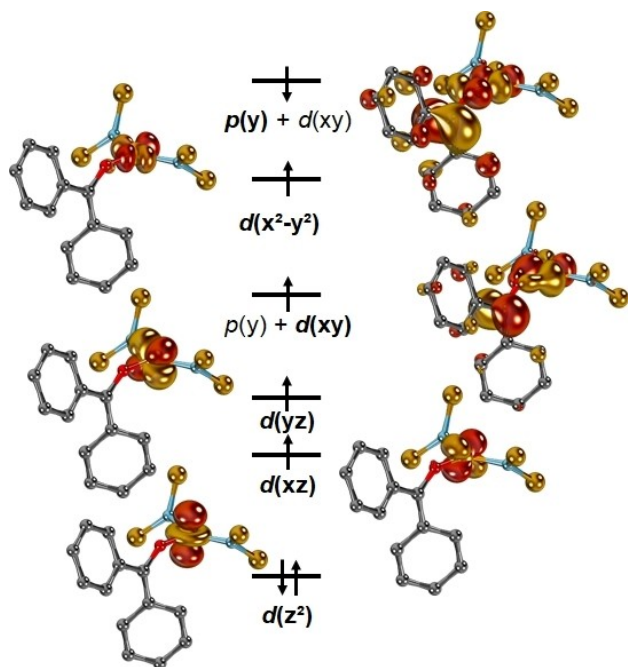


**Figure 6.** Molecular frontier orbitals<sup>1</sup> of  $[1]^-$  as obtained at the CASSCF (11,10) level of theory. Two doubly occupied and the related unoccupied, ligand-centred orbitals are omitted for clarity.

<sup>1</sup> For a thorough benchmark regarding structural parameters and absorption spectra, see Table S2–S9, S11 and Figure S61–S71.

**Table 3.** Calculated C–X resonances and bond lengths for benzophenone-coordinate complexes and comparison with free benzophenone (bp) and the anionic ketyl radical (bp<sup>•-</sup>).

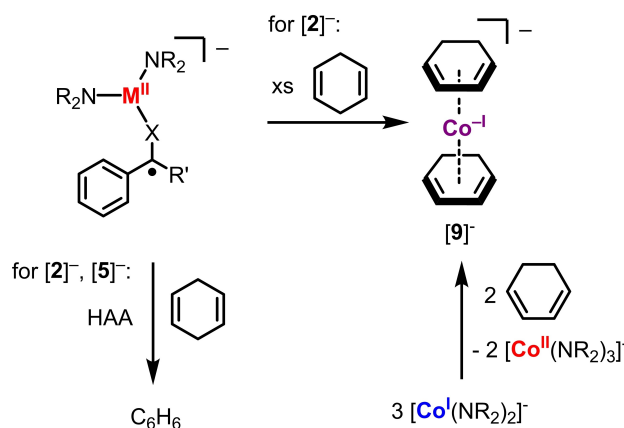
Compound	$\tilde{\nu}$ in $\text{cm}^{-1}$	C–O bond length in [Å]
Fe(bp <sup>•-</sup> ) ( $[1]^-$ )	1563	1.31
Co(bp <sup>•-</sup> ) ( $[2]^-$ )	1565	1.31
Fe(bp) (1)	1615	1.28
Co(bp) (2)	1590	1.27
bp <sup>•-</sup>	1536	1.27
bp	1701	1.23

to 1–3 and 6, thus corroborating a substantially reduced bond order and bond strength. For example, the C–O stretch is computed to resonate at  $1563 \text{ cm}^{-1}$  in  $[1]^-$  (C–O: 1.31 Å), at  $1565 \text{ cm}^{-1}$  in  $[2]^-$  (C–O: 1.31 Å), and at  $1536 \text{ cm}^{-1}$  for the “free” anionic benzophenone radical (C–O: 1.27 Å). In contrast, these stretches occur at considerably higher energies for the neutral congeners 1 ( $\tilde{\nu} = 1615 \text{ cm}^{-1}$ ; C–O: 1.28 Å) and 2 ( $\tilde{\nu} = 1590 \text{ cm}^{-1}$ ; C–O: 1.27 Å) as well as free benzophenone ( $\tilde{\nu} = 1701 \text{ cm}^{-1}$ ; C–O: 1.23 Å).

## Reactivity

Having established the substrate based radical character of the anionic compounds we were interested in how this would translate into radical-like reactivity, namely H atom abstraction (HAA) capability. The iron ketyl complex  $[1]^-$  showed no reaction with 1,4-cyclohexadiene (CHD). In contrast, CHD was dehydrogenated to benzene using the cobalt ketyl complex  $[2]^-$  and the iron aldimine complex  $[5]^-$  (Scheme 2).

This is accompanied by the appearance of new paramagnetic signals in the <sup>1</sup>H NMR spectroscopic analysis; unfortunately, the composition of the metal containing products (e.g. a metal(II) benzhydrolate) remained so far elusive. The presence of the radical anion in  $[2]^-$  and  $[5]^-$  is crucial as neither the metal(I) precursors nor the neutral complexes 2 and 3 facilitate the HAA of 1,4-CHD. Interestingly, using an excess of 1,4-CHD in



**Scheme 2.** Reactivity of  $[2]^-$  and  $[5]^-$  with 1,4-CHD and independent synthesis of  $[9]^-$ .

the presence of  $[2]^-$  led, besides some  $C_6H_6$ , to the formation of the anionic sandwich complex  $[Co^-(1,3-CHD)_2]^-$ ,  $[9]^-$ , and concomitantly  $[Co(NR_2)_3]^-$  which speaks to redox and ligand rearrangement.  $[9]^-$  resembles the related anthracenide or butadiene cobaltates(-I) from Ellis and co-workers (Scheme 2).<sup>[37]</sup> The presence of the ketyl ligand is thereby not necessary for the formation of  $[9]^-$  as it can be directly obtained via reaction of either 1,3- or 1,4-CHD and  $[Co(N(SiMe_3)_2)_2]^-$ . The formation of the 1,3-CHD complex  $[9]^-$  is accompanied by a sigmatropic H-atom shift of 1,4-CHD. The metal bound radical anions thus intriguingly act in two roles: a) as a facilitator for HAA abstraction and b) as an electron reservoir that reversibly masks a metal(I) ion. Next, we turned to the highly labile ketiminyl complexes  $[3]^-$  and  $[4]^-$ . Analysis of the decomposition of  $[3]^-$  revealed the formation of the homoleptic dinuclear iron(II) ketiminato complex  $[(L_2Fe)_2(\mu-L)_2]^{2-}$ ,  $[10]^{2-}$  (Scheme 3, Figure S95), which is likely the product of intermediate  $[Fe(NR_2)_3]^-$  followed by deprotonation of the liberated ketimine ( $L=N=CPh_2$ ).

No HAA abstraction was observed when treating  $[3]^-$  with 1,4-CHD. More intriguingly, the cobalt ketiminyl complex  $[4]^-$  transformed slowly into the dinuclear compound  $[11]^{2-}$  with deprotonation of the NH function as well as orthometallation of the ketimine ligand (Scheme 4, Figure S96). *In-situ*  $^1H$  NMR spectroscopy showed the further formation of  $HN(SiMe_3)_2$  and  $[Co(N(SiMe_3)_2)_3]^-$  which indicated an interplay of redox disproportionation and intramolecular deprotonation for the formation of  $[11]^{2-}$ . In contrast, in the presence of 1,4-CHD  $[4]^-$  slowly converts into the binuclear cobalt compound  $[12]^-$  (Figure S97) which forms as the result of a multitude of bond formation and cleavage processes. A now bridging ketimine was deprotonated at the nitrogen atom with additional C–C bond formation in *ortho*- $C_{aryl}$ -H position with the employed 1,4-CHD, that binds as a rearranged 1,3-cyclohexadienyl unit to one of the cobalt ions via the butadiene moiety. The coordination sphere of this cobalt ion is completed by a second ketimine that binds in a  $\eta_2$ -

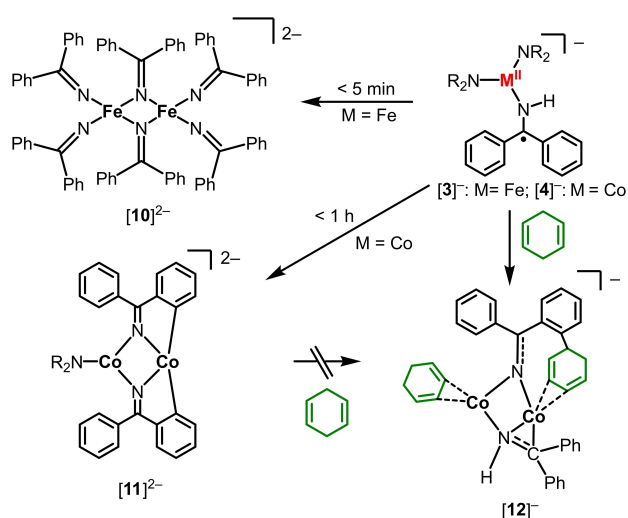
$\kappa^2$ -N: $\kappa^1$ -C fashion, whereas the C–N bond lengths of 1.396(5) Å speaks for a partially reduced state. The second cobalt ion is ligated by a 1,3-CHD ligand in addition to the two ketimine ligands. It is interesting to note that  $[12]^-$  is not a subsequent product of  $[11]^{2-}$  but of an unknown intermediate. The observed orthometallation of a ketone or imine linked arene is reminiscent of directing group assisted C–H bond functionalisation.<sup>[38,39]</sup> This is catalysed by a variety of metals, including cobalt. In these instances the directing group acts as a donor ligand and the C–H bond is broken either via deprotonation for high-valent<sup>[40]</sup> or oxidative addition and metal hydride formation for low-valent<sup>[39]</sup> cobalt species. In the presented case of  $[11]^{2-}$  and  $[12]^-$  the mechanism is not fully understood, but resembles imine activation by a Zr/Co-complex involving a cobalt hydride.<sup>[11]</sup> Eventually, the highly basic  $N(SiMe_3)_2$  ligands likely assists in a concerted metalation-deprotonation type pathway.

## Conclusion

We reported on the reduction of a diarylketone (benzophenone), a ketimine (ketimine benzophenone imine), as well as of a phenylaldimine (aldimine benzaldehyde methylamine) by anionic linear metal(I) complexes of iron and cobalt. Besides rare examples of ketyl radical anion complexes, this leads to the first structurally authenticated ketiminyl and aldiminyl radical metal compounds. The electronic description of a metal(II) bound radical anion is supported by comprehensive analysis of the structural, spectroscopic and physical properties of these compounds, and corroborated by quantum chemical calculations. We further revealed the multifaceted chemical behaviour of the high-spin complexes, which show H atom abstraction capability, reversible substrate reduction and coordination as well as, in case of cobalt, intramolecular C–H bond activation and dehydrogenative C–C bond formation via double C–H bond activation.

## Experimental Section

Details concerning the syntheses of all complexes, the spectroscopic and physical properties, *in situ* spectroscopic data and X-ray diffraction data are given in the Supporting Information. Deposition Numbers 2093093 ([K{18c6}][1]), 2093094 ([K{18c6}][2]), 2093095 (K{18c6}[3]), 2093096 (K{18c6}[4]), 2093097 (K{18c6}[5]), 2093086 (1), 2093087 (2), 2093088 (5), 2093089 (6), 2093090 (7), 2093091 (8), 2093098 (K{18c6}[9]), 2093099 ([K{18c6}][10]), 2093100 ([K{18c6}][11]), 2093092 (K{18c6}[12]) contain the supplementary crystallographic data for this paper. These data are provided free of charge by the joint Cambridge Crystallographic Data Centre and Fachinformationszentrum Karlsruhe Access Structures service.<sup>2</sup>



**Scheme 3.** Further conversion of  $[3]^-$  and  $[4]^-$  and its reactivity towards 1,4-CHD.

<sup>2</sup> Molecular orbitals were plotted with IBOView *J. Chem. Theory Comput.* **2013**, *9*, 4834.

## Acknowledgements

C.G.W. thanks the Deutsche Forschungsgemeinschaft (WE 5627/4-1), the Fond der Chemischen Industrie and the Philipps-University for financial support. D.M. thanks the RRZ Erlangen for computational resources. We thank J. Lange (I. Physikalisches Institut, Univ. Gießen) for the acquisition of the EPR data. Open Access funding enabled and organized by Projekt DEAL.

## Conflict of Interest

The authors declare no conflict of interest.

**Keywords:** cobalt · iron · radical anions · quantum chemical calculation · spectroscopy

- [1] a) E. Clemmensen, *Ber. Dtsch. Chem. Ges.* **1913**, *46*, 1837; b) M. L. Di Vona, V. Rosnati, *J. Org. Chem.* **1991**, *56*, 4269; c) J. G. C. St. Buchanan, P. D. Woodgate, *Q. Rev. Chem. Soc.* **1969**, *23*, 522; d) E. Vedejs in *Organomet. React.*, Wiley Online Library, [Hoboken, N. J.], **2004**, pp. 401–422; e) J. H. Brewster, *J. Am. Chem. Soc.* **1954**, *76*, 6364; f) T. Wirth, *Angew. Chem. Int. Ed.* **1996**, *35*, 61; g) M. Ephritikhine, *Chem. Commun.* **1998**, 2549; h) M. Ephritikhine, C. Villiers in *Modern Carbonyl Olefination* (Ed.: T. Takeda), Wiley-VCH, Weinheim, **2004**, pp. 223–285.
- [2] R. D. Rieke, S.-H. Kim, *J. Org. Chem.* **1998**, *63*, 5235.
- [3] Á. Péter, S. Agasti, O. Knowles, E. Pye, D. J. Procter, *Chem. Soc. Rev.* **2021**, *50*, 5349.
- [4] a) M. Szostak, M. Spain, A. J. Eberhart, D. J. Procter, *J. Am. Chem. Soc.* **2014**, *136*, 2268; b) D. Parmar, L. A. Duffy, D. V. Sadasivam, H. Matsubara, P. A. Bradley, R. A. Flowers, D. J. Procter, *J. Am. Chem. Soc.* **2009**, *131*, 15467; c) M. Szostak, B. Sautier, M. Spain, M. Behlendorf, D. J. Procter, *Angew. Chem. Int. Ed.* **2013**, *52*, 12559.
- [5] a) O. Ishitani, C. Pac, H. Sakurai, *J. Org. Chem.* **1983**, *48*, 2941; b) K. T. Tarantino, P. Liu, R. R. Knowles, *J. Am. Chem. Soc.* **2013**, *135*, 10022; c) L. J. Rono, H. G. Yayla, D. Y. Wang, M. F. Armstrong, R. R. Knowles, *J. Am. Chem. Soc.* **2013**, *135*, 17735; d) M. Nakajima, E. Fava, S. Loeschner, Z. Jiang, M. Rueping, *Angew. Chem. Int. Ed.* **2015**, *54*, 8828; e) S. Wang, N. Lokesh, J. Hioe, R. M. Gschwind, B. König, *Chem. Sci.* **2019**, *10*, 4580; f) D. Hager, D. W. C. MacMillan, *J. Am. Chem. Soc.* **2014**, *136*, 16986; g) M. Li, S. Berritt, L. Matuszewski, G. Deng, A. Pascual-Escudero, G. B. Panetti, M. Poznik, X. Yang, J. J. Chruma, P. J. Walsh, *J. Am. Chem. Soc.* **2017**, *139*, 16327; h) C. K. Prier, D. A. Rankic, D. W. C. MacMillan, *Chem. Rev.* **2013**, *113*, 5322; i) S. Wang, B. König, *Angew. Chem. Int. Ed.* **2021**, 10.1002/anie.202105469.
- [6] a) E. J. Enholm, M. A. Battiste, M. Gallagher, K. M. Moran, A. Alberti, M. Guerra, D. Macciantelli, *J. Org. Chem.* **2002**, *67*, 6579; b) J. E. Bennett, B. Mile, A. Thomas, *J. Chem. Soc. A* **1968**, 0, 298; c) A. G. Davies, A. G. Neville, *J. Chem. Soc. Perkin Trans. 2* **1992**, 163; d) R. Koeppe, P. H. Kasai, *J. Phys. Chem.* **1994**, *98*, 12904; e) A. G. Evans, J. C. Evans, P. J. Emes, S. I. Haider, *J. Chem. Soc. Perkin Trans. 2* **1974**, 1121; f) K. J. Covert, P. T. Wolczanski, S. A. Hill, P. J. Krusic, *Inorg. Chem.* **1992**, *31*, 66; g) H. Zhang, B. Wu, S. L. Marquard, E. D. Litle, D. A. Dickie, M. W. Bezpalko, B. M. Foxman, C. M. Thomas, *Organometallics* **2017**, *36*, 3498; h) M. Shit, S. Bera, S. Maity, T. Weyhermüller, P. Ghosh, *New J. Chem.* **2017**, *41*, 4564; i) N. Hirota, S. I. Weissman, *J. Am. Chem. Soc.* **1964**, *86*, 2538.
- [7] T. A. Scott, B. A. Ooro, D. J. Collins, M. Shatruk, A. Yakovenko, K. R. Dunbar, H.-C. Zhou, *Chem. Commun.* **2009**, 65.
- [8] H. Bock, H.-F. Herrmann, D. Fenske, H. Goesmann, *Angew. Chem. Int. Ed.* **1988**, *27*, 1067.
- [9] J. C. Ott, H. Wadepohl, L. H. Gade, *Angew. Chem.* **2020**, *132*, 9535.
- [10] Z. Hou, A. Fujita, T. Koizumi, H. Yamazaki, Y. Wakatsuki, *Organometallics* **1999**, *18*, 1979.
- [11] S. L. Marquard, M. W. Bezpalko, B. M. Foxman, C. M. Thomas, *Organometallics* **2014**, *33*, 2071.
- [12] a) G. A. Molander, C. R. Harris, *Chem. Rev.* **1996**, *96*, 307; b) Z. Hou, A. Fujita, H. Yamazaki, Y. Wakatsuki, *J. Am. Chem. Soc.* **1996**, *118*, 2503; c) A. Domingos, I. Lopes, J. C. Waerenborgh, N. Marques, G. Y. Lin, X. W. Zhang, J. Takats, R. McDonald, A. C. Hillier, A. Sella et al., *Inorg. Chem.* **2007**, *46*, 9415.
- [13] Z. Hou, T. Koizumi, M. Nishiura, Y. Wakatsuki, *Organometallics* **2001**, *20*, 3323.
- [14] Z. Hou, A. Fujita, H. Yamazaki, Y. Wakatsuki, *J. Am. Chem. Soc.* **1996**, *118*, 7843.
- [15] Z. Hou, T. Miyano, H. Yamazaki, Y. Wakatsuki, *J. Am. Chem. Soc.* **1995**, *117*, 4421.
- [16] Z. Hou, A. Fujita, Y. Zhang, T. Miyano, H. Yamazaki, Y. Wakatsuki, *J. Am. Chem. Soc.* **1998**, *120*, 754.
- [17] O. P. Lam, C. Anthon, F. W. Heinemann, J. M. O'Connor, K. Meyer, *J. Am. Chem. Soc.* **2008**, *130*, 6567.
- [18] C. Jones, L. McDyre, D. M. Murphy, A. Stasch, *Chem. Commun.* **2010**, 46, 1511.
- [19] Z. Hou, X. Jia, A. Fujita, H. Tezuka, H. Yamazaki, Y. Wakatsuki, *Chem. Eur. J.* **2000**, *6*, 2994.
- [20] a) K. J. Covert, P. T. Wolczanski, *Inorg. Chem.* **1989**, *28*, 4565; b) S. L. Marquard, M. W. Bezpalko, B. M. Foxman, C. M. Thomas, *J. Am. Chem. Soc.* **2013**, *135*, 6018; c) W. Zhou, S. L. Marquard, M. W. Bezpalko, B. M. Foxman, C. M. Thomas, *Organometallics* **2013**, *32*, 1766; d) F. Ortu, J. Liu, P. C. Junk, J. M. Fowler, A. Formanuk, M.-E. Boulon, N. F. Chilton, D. P. Mills, *Inorg. Chem.* **2017**, *56*, 2496; e) C. A. P. Goodwin, N. F. Chilton, G. F. Vettese, E. Moreno Pineda, I. F. Crowe, J. W. Ziller, R. E. P. Winpenny, W. J. Evans, D. P. Mills, *Inorg. Chem.* **2016**, *55*, 10057; f) G. B. Deacon, P. C. Junk, J. Wang, D. Werner, *Inorg. Chem.* **2014**, *53*, 12553; g) I. L. Fedushkin, A. A. Skatova, V. K. Cherkasov, V. A. Chudakova, S. Dechert, M. Hummert, H. Schumann, *Chem. Eur. J.* **2003**, *9*, 5778; h) G. B. Deacon, C. M. Forsyth, D. L. Wilkinson, *Chem. Eur. J.* **2001**, *7*, 1784.
- [21] K. C. Mullane, T. Cheisson, E. Nakamaru-Ogiso, B. C. Manor, P. J. Carroll, E. J. Schelter, *Chem. Eur. J.* **2018**, *24*, 826.
- [22] a) Z. Flisak, W.-H. Sun, *ACS Catal.* **2015**, *5*, 4713; b) V. C. Gibson, C. Redshaw, G. A. Solan, *Chem. Rev.* **2007**, *107*, 1745; c) K. G. Caulton, *Eur. J. Inorg. Chem.* **2012**, 2012, 435; d) S. Blanchard, E. Derat, M. Desage-El Murr, L. Fensterbank, M. Malacria, V. Mouries-Mansuy, *Eur. J. Inorg. Chem.* **2012**, 2012, 376; e) N. J. Hill, I. Vargas-Baca, A. H. Cowley, *Dalton Trans.* **2009**, 240; f) I. L. Fedushkin, A. A. Skatova, V. A. Chudakova, G. K. Fukin, *Angew. Chem. Int. Ed.* **2003**, *42*, 3294; g) T. M. Maier, M. Gawron, P. Coburger, M. Bodensteiner, R. Wolf, N. P. van Leest, B. de Bruin, S. Demeshko, F. Meyer, *Inorg. Chem.* **2020**, *59*, 16035; h) T. M. Maier, S. Sandl, I. G. Shenderovich, A. Jacobi von Wangelin, J. J. Weigand, R. Wolf, *Chem. Eur. J.* **2019**, *25*, 238; i) C. C. Lu, T. Weyhermüller, E. Bill, K. Wiegardt, *Inorg. Chem.* **2009**, *48*, 6055; j) W. N. Palmer, T. Diao, I. Pappas, P. J. Chirik, *ACS Catal.* **2015**, *5*, 622; k) C. C. Lu, E. Bill, T. Weyhermüller, E. Bothe, K. Wiegardt, *J. Am. Chem. Soc.* **2008**, *130*, 3181.
- [23] A. Reckziegel, C. Pietzonka, F. Kraus, C. G. Werncke, *Angew. Chem. Int. Ed.* **2020**, *59*, 8527.
- [24] C. G. Werncke, P. C. Bunting, C. Duhayon, J. R. Long, S. Bontemps, S. Sabo-Etienne, *Angew. Chem.* **2015**, *127*, 247.
- [25] C. G. Werncke, E. Suturina, P. C. Bunting, L. Vendier, J. R. Long, M. Atanasov, F. Neese, S. Sabo-Etienne, S. Bontemps, *Chem. Eur. J.* **2016**, *22*, 1668.
- [26] S. Yao, C. Milsman, E. Bill, K. Wiegardt, M. Driess, *J. Am. Chem. Soc.* **2008**, *130*, 13536.
- [27] a) S. Camadanli, R. Beck, U. Flörke, H.-F. Klein, *Organometallics* **2009**, *28*, 2300; b) S. Yogendra, T. Weyhermüller, A. W. Hahn, S. DeBeer, *Inorg. Chem.* **2019**, *58*, 9358.
- [28] I. Müller, C. Schneider, C. Pietzonka, F. Kraus, C. G. Werncke, *Inorganics* **2019**, *7*, 117.
- [29] a) I. Müller, C. G. Werncke, *Chem. Eur. J.* **2021**, *27*, 4932; b) C. G. Werncke, I. Müller, *Chem. Commun.* **2020**, 56, 2268; c) C. G. Werncke, J. Pfeiffer, I. Müller, L. Vendier, S. Sabo-Etienne, S. Bontemps, *Dalton Trans.* **2019**, 48, 1757.
- [30] I. Müller, D. Munz, C. G. Werncke, *Inorg. Chem.* **2020**, *59*, 9521.
- [31] A. Eichhöfer, Y. Lan, V. Mereacre, T. Bodenstein, F. Weigend, *Inorg. Chem.* **2014**, *53*, 1962.
- [32] a) K. Ding, T. R. Dugan, W. W. Brennessel, E. Bill, P. L. Holland, *Organometallics* **2009**, *28*, 6650; b) A. Reckziegel, M. Kour, B. Battistella, S. Mebs, K. Beuthert, R. Berger, C. G. Werncke, *Angew. Chem. Int. Ed.* **2021**, *60*, 15376; c) P. Pietrzyk, M. Srebro, M. Radoń, Z. Sojka, A. Michalak, *J. Phys. Chem. A* **2011**, *115*, 2316.
- [33] V. Lyaskovskyy, A. I. O. Suarez, H. Lu, H. Jiang, X. P. Zhang, B. de Bruin, *J. Am. Chem. Soc.* **2011**, *133*, 12264.
- [34] a) J. C. Ott, H. Wadepohl, L. H. Gade, *Angew. Chem. Int. Ed.* **2020**, *59*, 9448; b) K. P. Chiang, S. M. Bellows, W. W. Brennessel, P. L. Holland,

- Chem. Sci.* **2014**, *5*; c) J. M. Smith, A. R. Sadique, T. R. Cundari, K. R. Rodgers, G. Lukat-Rodgers, R. J. Lachicotte, C. J. Flaschenriem, J. Vela, P. L. Holland, *J. Am. Chem. Soc.* **2006**, *128*, 756; d) J. J. Kiernicki, J. P. Shanahan, M. Zeller, N. K. Szymczak, *Chem. Sci.* **2019**, *10*, 5539; e) K. P. Chiang, C. C. Scarborough, M. Horitani, N. S. Lees, K. Ding, T. R. Dugan, W. W. Brennessel, E. Bill, B. M. Hoffman, P. L. Holland, *Angew. Chem. Int. Ed.* **2012**, *51*, 3658.
- [35] a) F. Neese, *WIREs Comput. Mol. Sci.* **2012**, *2*, 73; b) F. Neese, *WIREs Comput. Mol. Sci.* **2018**, *8*.
- [36] a) B. O. Roos, P. R. Taylor, P. E. Sigbahn, *Chem. Phys.* **1980**, *48*, 157; b) C. Angeli, R. Cimiraaglia, S. Evangelisti, T. Leininger, J.-P. Malrieu, *J. Chem. Phys.* **2001**, *114*, 10252.
- [37] W. W. Brennessel, J. V. G. Young, J. E. Ellis, *Angew. Chem. Int. Ed.* **2002**, *41*, 1211.
- [38] a) K. Gao, N. Yoshikai, *Acc. Chem. Res.* **2014**, *47*, 1208; b) P.-S. Lee, N. Yoshikai, *Org. Lett.* **2015**, *17*, 22; c) S. M. Ujwaldev, N. A. Harry, M. A. Divakar, G. Anilkumar, *Catal. Sci. Technol.* **2018**, *8*, 5983; d) Y. Lian, T. Huber, K. D. Hesp, R. G. Bergman, J. A. Ellman, *Angew. Chem. Int. Ed.* **2013**, *52*, 629; e) Y. Lian, R. G. Bergman, L. D. Lavis, J. A. Ellman, *J. Am. Chem. Soc.* **2013**, *135*, 7122; f) E. Nakamura, N. Yoshikai, *J. Org. Chem.* **2010**, *75*, 6061; g) K. Gao, P.-S. Lee, T. Fujita, N. Yoshikai, *J. Am. Chem. Soc.* **2010**, *132*, 12249; h) S. Murahashi, *J. Am. Chem. Soc.* **1955**, *77*, 6403.
- [39] B. J. Fallon, J.-B. Garsi, E. Derat, M. Amatore, C. Aubert, M. Petit, *ACS Catal.* **2015**, *5*, 7493.
- [40] a) J. R. Hummel, J. A. Ellman, *J. Am. Chem. Soc.* **2015**, *137*, 490; b) T. Yoshino, H. Ikemoto, S. Matsunaga, M. Kanai, *Angew. Chem. Int. Ed.* **2013**, *52*, 2207.

---

Manuscript received: August 25, 2021

Accepted manuscript online: September 27, 2021

Version of record online: October 22, 2021